Consistent Lattice Boltzmann schemes for gas mixture modeling in the low Mach number limit

Pietro Asinari, PhD

Department of Energetics, Politecnico di Torino

WORKSHOP GALILEO 2007, 5 – 6 October 2007,
Department of Mathematics, Università di Parma, Italy

Outline of this talk

1. Lattice Boltzmann Method
   - Mesoscopic Numerical Methods for ICNS
   - Microscopic Velocity Discretization
   - Space and Time Discretization
2. Homogeneous mixture flow modeling
   - Mixture characterization
   - Macroscopic modeling
   - Kinetic modeling
3. LBM scheme for mixture modeling
   - Simplified AAP model
   - Design of the discrete local equilibrium
   - Numerical results

Outline Compass

Mesoscopic Numerical Methods for ICNS

Most of LBM models points to kinetic equations in order to solve fluidynamic equations in continuous regime (Incompressible Navier-Stokes – ICNS) ? Does it worth the effort ?

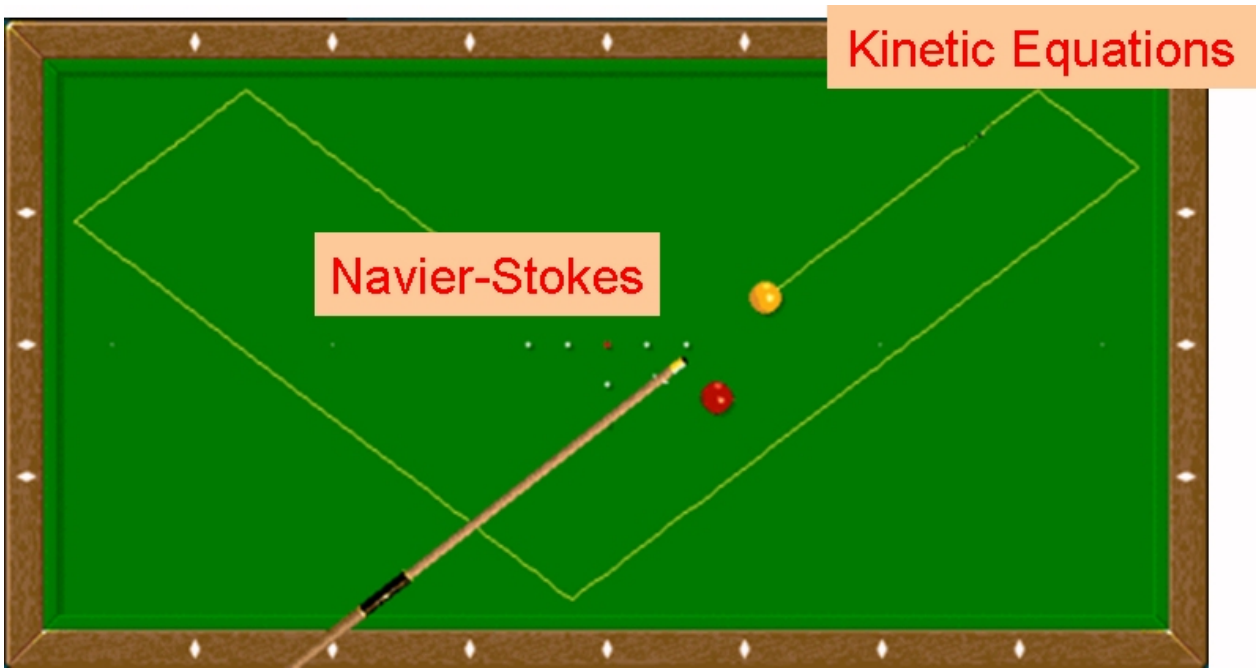

Main Categories

- Mesoscopic methods may be distinguished in two main categories:
  - (**Primitive**) Numerical methods using expressions for the numerical fluxes, derived by simplified solutions of kinetic equations (equilibrium and/or small-deviation solutions), for example GKS $\rightarrow$ they are not truly kinetic schemes, because the kinetic expressions are used for physically-based macroscopic averaging
  - (**Kinetic**) Numerical methods formulated directly in terms of kinetic variables, for example LBM $\rightarrow$ they are truly kinetic schemes, if and only if the adopted discretization allows to catch the kinetic phenomena, otherwise their kinetic content is questionable

Lattice Boltzmann Method (LBM) in a Nutshell

- number of papers on International Journals: 2,000 in the period 1988-2007 (for comparison, 28,000 papers on "Energy Saving"...)
- number of books: 14 in the period 2000-2007
- main international conferences:
  - International Conference on Mesoscopic Methods in Engineering and Science, ICMMES
  - Discrete Simulation of Fluid Dynamics in Complex Systems, DSFD
- commercial codes: PowerFLOW (EXA, spin-off MIT)
- patents: mainly in bio-fluidics for medical applications

Simplified BGK Model Equation

In the incompressible continuum limit, the Mach number as well as the Knudsen number is vanishingly small and the deviations of temperature and density are vanishingly small. Then, we can employ the simplified BGK equation, i.e.

- the isothermal equilibrium distribution $f_e^* \rightarrow f_e$, namely

$$f_e = \frac{\rho}{2\,\pi/3}\,\exp\left[-\frac{3(\xi_i - u_i)^2}{2}\right], \tag{1}$$

  where $m = 1$ (since it is a constant), $d = 2$ (for two dimensional case) and $e = 1/3$ are assumed;
- and the collision frequency independent of the local state, namely $\lambda(\rho) \rightarrow \lambda$.

Gaussian Quadratures

We need to accurately compute integrals such as $\ll \phi(\boldsymbol{\xi}) f_e \gg$: in particular, for the hydrodynamic conserved moments $\phi = 1, \xi_i$. The previous integrals can be expressed as

$$\ll \phi(\boldsymbol{\xi}) f_e \gg = \frac{\rho}{\pi} \int \phi(\boldsymbol{\xi}) \exp\left[-(\boldsymbol{\xi}^* - \boldsymbol{u})^2\right] \, d\xi_x^* d\xi_y^*, \qquad (2)$$

where $d\xi_i^* = d\xi_i \sqrt{3/2}$. Let us apply a Gaussian quadrature in order to numerically solve the previous integrals by means of N discrete point along each direction

$$\ll \phi(\boldsymbol{\xi}) f_e \gg = \sum_{i=1}^{N} \sum_{j=1}^{N} \left(\zeta_i \zeta_j \, \phi \, f_e\right) \left(\xi_x^* = \xi_i^*, \xi_y^* = \xi_j^*\right) + E_N, \qquad (3)$$

where ζ_i and ζ_i are proper weighting functions.

(1) Three-point Gauss-Hermite Formula

Let us rewrite the previous expression as

$$\ll \phi(\boldsymbol{\xi}) f_e \gg = \frac{\rho}{\pi} \int \psi(\boldsymbol{\xi}^*) \exp\left[-(\boldsymbol{\xi}^*)^2\right] \, d\xi_x^* d\xi_y^*, \tag{4}$$

where $\psi(\boldsymbol{\xi}^*) = \phi(\boldsymbol{\xi}) \exp\left[-\boldsymbol{u} \cdot (\boldsymbol{u} + 2\boldsymbol{\xi}^*)\right]$. Because of the weighting factor, among all the Gaussian quadratures, it is convenient to adopt the Gauss-Hermite formula. For example, in the case of the three-point formula, the three abscissas and the corresponding weighting functions of the quadrature are

$$\xi_1^* = -\sqrt{3/2} \;\; , \;\; \xi_2^* = 0 \;\; , \;\; \xi_3^* = +\sqrt{3/2} \, , \tag{5}$$

and $\zeta_i = w_i \exp\left[(\xi_i^*)^2\right]$ respectively, where

$$w_1 = \sqrt{\pi}/6 \;\; , \;\; w_2 = 2\sqrt{\pi}/3 \;\; , \;\; w_3 = \sqrt{\pi}/6 \, . \tag{6}$$

Obviously three points are very few and large E_N is expected.

(2) Incompressible Limit

The low Mach number limit $|\boldsymbol{u}| \ll |\boldsymbol{\xi}|$ allows one to expand $\psi = \psi_0 + O(\boldsymbol{u}^3)$, where

$$\psi_0(\boldsymbol{\xi}^*) = \phi(\boldsymbol{\xi}) \left[1 - \boldsymbol{u} \cdot (\boldsymbol{u} + 2\,\boldsymbol{\xi}^*) + 2\,(\boldsymbol{u} \cdot \boldsymbol{\xi}^*)\right]. \tag{7}$$

In the following, the truncated expansion ψ_0 will be used instead of ψ. In case of the hydrodynamic moments $\phi = 1, \xi_i$, the quadrature formula yields

$$\ll f_e \gg = \rho \sum_{i=1}^{3}\sum_{j=1}^{3} W_{i\,j}\, \psi_0(\xi_x^* = \xi_i^*, \xi_y^* = \xi_j^*) = \rho, \tag{8}$$

$$\ll \boldsymbol{\xi} f_e \gg = \rho \sum_{i=1}^{3}\sum_{j=1}^{3} W_{i\,j}\, (\boldsymbol{\xi}\,\psi_0)(\xi_x^* = \xi_i^*, \xi_y^* = \xi_j^*) = \rho \boldsymbol{u}. \tag{9}$$

where $W_{i\,j} = w_i w_j/\pi$. In this case, the error E_N is zero !!

D2Q9 Lattice Definition

- The previous unexpected result is valid for all ϕ up to second order with regards to the particle velocities: higher order moments show the limits of the poor quadrature formula in terms of its symmetry properties and the numerical calculation is not exact any more
- Let us rearrange the velocities of the quadrature formula $\{(\xi_x^* = \xi_i^*, \xi_y^* = \xi_j^*)|i,j = 1,2,3\}$ in a finite set of $Q = 9$ particle velocities, called D2Q9 lattice, i.e. equivalently $\{\boldsymbol{\xi}_q|0 \leq q \leq (Q-1)\}$, and let us collect the velocity components in a second order tensor $\boldsymbol{V}$, i.e. $\boldsymbol{V} = [\boldsymbol{\xi}_0, \boldsymbol{\xi}_1, \cdots \boldsymbol{\xi}_{(Q-1)}]^T$. The result is very simple, namely

$$\boldsymbol{V}^T = \begin{bmatrix} 0 & 1 & 0 & -1 & 0 & 1 & -1 & -1 & 1 \\ 0 & 0 & 1 & 0 & -1 & 1 & 1 & -1 & -1 \end{bmatrix}. \quad (10)$$

(3) Local Equilibrium Definition

- Let us introduce a new definition of local equilibrium for the considered lattice as a vector of polynomials $\boldsymbol{f}_e \in \mathbb{R}^9$, defined in such a way that the generic component q is

$$(\boldsymbol{f}_e)_q = \rho\, W_q\, \psi_0(\xi_x = V_{q\,1}, \xi_y = V_{q\,2}). \tag{11}$$

- Moreover let us introduce the following discrete operator $< \cdot, \cdot >$, which involves a sum on the lattice discrete velocities, namely

$$< A_{i\ j\,\ldots\,q}, B_{m\ n\,\ldots\,q} >= \sum_{q=0}^{Q} A_{i\ j\,\ldots\,q}\, B_{m\ n\,\ldots\,q} = C_{i\,j\,m\,n\,\ldots}.$$

- Hence the previous results can be expressed as $\ll f_e \gg =< 1, \boldsymbol{f}_e >= \rho$ and $\ll \boldsymbol{\xi} f_e \gg =< \boldsymbol{V}, \boldsymbol{f}_e >= \rho \boldsymbol{u}$

(4) Method of Characteristics (MOC)

- In the discretization of the lattice BGK equation, let us apply the method of characteristics (MOC) $\rightarrow$ Let us consider the streamlines defined by the condition $V_{q\,i} = d\hat{x}_i/d\hat{t}$, i.e. $\hat{x}^*_i(\hat{t}) = V_{q\,i}\,(\hat{t} - \hat{t}_0) + \hat{x}^*_{i\,0}$, where $\hat{x}^*_{i\,0}$ is a proper constant
- Along these streamlines, the following notation holds

$$\frac{\partial f_q}{\partial \hat{t}} + V_{q\,1}\frac{\partial f_q}{\partial \hat{x}_1} + V_{q\,2}\frac{\partial f_q}{\partial \hat{x}_2} = \sum_{\alpha \in A} \frac{\partial f_q}{\partial \hat{\alpha}}\frac{d\hat{\alpha}}{d\hat{t}} = \frac{D f_q}{D\hat{t}} = \lambda(f_{e\,q} - f_q), \tag{12}$$

  where $A = \{\hat{t}, \hat{x}_1, \hat{x}_2\}$.
- The theory of characteristics for this case is extremely simplified, because $\boldsymbol{V}$ is made of constants, and in particular $|V_{q\,i}| = 0, 1$ for $\forall q, i$

Forward Euler Time Integration Formula

- Let us introduce an homogeneous space discretization with $\delta\hat{x}$ spacing and let $\hat{x}^*_{i\,0}$ be a discretization grid node
- If the time discretization step is assumed $\delta\hat{t} = \delta\hat{x}$, then moving along the previously defined characteristic yields $\hat{x}^*_i(n) = n\,h\,V_{q\,i} + \hat{x}^*_{i\,0}$ and, taking into account that $|V_{q\,i}| = 0, 1$ for $\forall q, i$, then $\hat{x}^*_i(n)$ is again a discretization grid node at any discrete time
- During an elementary time step, the particles jump to the neighboring nodes according to their discrete velocity
- Applying the forward Euler time integration formula to the discrete BGK equation and taking $\delta\hat{t} = 1$ yields the simplest LBM scheme

$$f_q(\hat{t}+1, \hat{x}_i) = f_q(\hat{t}, \hat{x}_i - V_{q\,i}) + \lambda\,(f_{e\,q} - f_q)(\hat{t}, \hat{x}_i - V_{q\,i}). \quad (13)$$

Outline Compass

Concentration measures

- The mass concentration is defined as

$$x_\sigma = \rho_\sigma / \rho, \tag{14}$$

where ρ_σ is the single species density, while $\rho = \sum_\varsigma \rho_\varsigma$ is the total mixture density.

- The molar density as

$$n_\sigma = \rho_\sigma / m_\sigma, \tag{15}$$

where m_σ is the molecular weight, i.e. the weight of one mole of molecules.

- Consequently the molar concentration as

$$y_\sigma = n_\sigma / n, \tag{16}$$

where $n = \sum_\varsigma n_\varsigma$ is the total mixture *molar* density.

Mixture velocities

- The mass-averaged mixture velocity is defined as

$$\boldsymbol{u} = \sum_{\varsigma} x_{\varsigma} \boldsymbol{u}_{\varsigma}, \tag{17}$$

where $\boldsymbol{u}_{\varsigma}$ is the single species velocity. Since the *mass* concentrations where used, the previous quantity is also called barycentric (mixture) velocity.

- Similarly, by means of the molar concentrations, it is possible to define a mole-averaged mixture velocity, namely

$$\boldsymbol{v} = \sum_{\varsigma} y_{\varsigma} \boldsymbol{u}_{\varsigma}. \tag{18}$$

Since the *molar* concentrations where used, the previous quantity is also called molar (mixture) velocity.

Diffusion fluxes

- It is possible to define a specific mass diffusion flux for each species σ as

$$\boldsymbol{j}_\sigma = \rho_\sigma \boldsymbol{w}_\sigma, \tag{19}$$

where $\boldsymbol{w}_\sigma = \boldsymbol{u}_\sigma - \boldsymbol{u}$ is the *mass* diffusion velocity and clearly $\sum_\varsigma \boldsymbol{j}_\varsigma = 0$.

- Similarly, it is possible to define a specific molar diffusion flux for each species σ as

$$\boldsymbol{k}_\sigma = n_\sigma \boldsymbol{z}_\sigma, \tag{20}$$

where $\boldsymbol{z}_\sigma = \boldsymbol{u}_\sigma - \boldsymbol{v}$ is the *molar* diffusion velocity and clearly $\sum_\varsigma \boldsymbol{k}_\varsigma = 0$.

Maxwell-Stefan model

- In case of more than two species, the diffusion fluxes can be described macroscopically by the Maxwell-Stefan model, namely

$$\nabla y_\sigma = \sum_\varsigma B_{\sigma\varsigma} y_\sigma y_\varsigma (\boldsymbol{u}_\varsigma - \boldsymbol{u}_\sigma) = \frac{1}{n} \sum_\varsigma B_{\sigma\varsigma} (y_\sigma \boldsymbol{k}_\varsigma - y_\varsigma \boldsymbol{k}_\sigma), \tag{21}$$

where $B_{\sigma\varsigma} = B(m_\sigma, m_\varsigma)$ is the binary Maxwell-Stefan diffusion resistance coefficient. An important comment is that the previous parameter only depends (according to the results of the kinetic theory) on the molecular weights of considered species and on the total pressure and (total) temperature (thermodynamic variables identifying the mixture equilibrium state).

Full Boltzmann equations

- The simultaneous Boltzmann equations for a mixture without external force can be written as:

$$\partial_{\hat{t}} f_\sigma + \boldsymbol{\xi} \cdot \hat{\boldsymbol{\nabla}} f_\sigma = Q_\sigma, \tag{22}$$

where $Q_\sigma = \sum_\varsigma Q_{\sigma\varsigma}$ and $Q_{\sigma\varsigma} = Q_{\varsigma\sigma}$, $\varsigma \neq \sigma$, is the cross collision term for two different species σ and ς. Obviously, for an N-component system, there will be N such equations. In general, the collision term is

$$Q_{\sigma\varsigma} = \int d\boldsymbol{\xi}_\varsigma d\Theta d\varepsilon B(\Theta, \|\boldsymbol{\xi}_{\sigma\varsigma}\|)[f'_\sigma f'_\varsigma - f_\sigma f_\varsigma], \tag{23}$$

where f'_σ (f'_ς) and f_σ (f_ς) denote the post-collision and pre-collision state of the particle of species σ (ς), respectively, $\boldsymbol{\xi}_{\sigma\varsigma} = \boldsymbol{\xi} - \boldsymbol{\xi}_\varsigma$.

Momentum transfer among the species

- Clearly the momentum of the single species is not conserved, because the species are interacting each other by transferring momentum, in such a way that the total mixture momentum is conserved.
- Hence it is worth the effort to compute the following integral, which describes the momentum transfer prescribed by full Boltzmann equations, namely

$$\int \boldsymbol{\xi} Q_\sigma d\boldsymbol{\xi} = p \sum_\varsigma B_{\sigma\varsigma} y_\sigma y_\varsigma (\boldsymbol{u}_\varsigma - \boldsymbol{u}_\sigma), \tag{24}$$

where now the Maxwell-Stefan diffusion resistance coefficient $B_{\sigma\varsigma}$ can be interpreted as macroscopic consequence of the interaction potential between species σ and ς.

Outline Compass

Simplified AAP model

- Let us consider a simplified version of the AAP model [Andries, Aoki, and Perthame 2002], which is based on only one global (i.e., taking into account all the species ς) operator for each species σ, namely

$$\partial_{\hat{t}} f_\sigma + \boldsymbol{\xi} \cdot \hat{\boldsymbol{\nabla}} f_\sigma = \lambda_\sigma \left[f_{\sigma(*)} - f_\sigma \right], \tag{25}$$

where

$$f_{\sigma(*)} = \frac{\rho_\sigma}{(2\pi\varphi_\sigma/3)} \exp\left[-\frac{3\,(\boldsymbol{\xi} - \boldsymbol{u}^*_\sigma)^2}{2\,\varphi_\sigma} \right], \tag{26}$$

and

$$\boldsymbol{u}^*_\sigma = \boldsymbol{u}_\sigma + \sum_\varsigma \frac{m^2}{m_\sigma m_\varsigma} \frac{B_{\sigma\varsigma}}{B_{\sigma\sigma}} x_\varsigma (\boldsymbol{u}_\varsigma - \boldsymbol{u}_\sigma). \tag{27}$$

Properties of simplified AAP model

- The target velocity can be easily recasted as

$$\boldsymbol{u}_\sigma^* = \boldsymbol{u} + \sum_\varsigma \left(\frac{m^2}{m_\sigma m_\varsigma} \frac{B_{\sigma\varsigma}}{B_{\sigma\sigma}} - 1 \right) x_\varsigma (\boldsymbol{u}_\varsigma - \boldsymbol{u}_\sigma). \tag{28}$$

- If $m_\sigma = m$ for $\forall \sigma$, then (Property 1)

$$\boldsymbol{u}_\sigma^* = \boldsymbol{u} + \sum_\varsigma \left(\frac{m^2}{mm} \frac{B_{mm}}{B_{mm}} - 1 \right) x_\sigma x_\varsigma (\boldsymbol{u}_\varsigma - \boldsymbol{u}_\sigma) = \boldsymbol{u}. \tag{29}$$

- Clearly (Property 2)

$$\sum_\sigma x_\sigma \boldsymbol{u}_\sigma^* = \boldsymbol{u} + \sum_\sigma \sum_\varsigma \left(\frac{m^2}{m_\sigma m_\varsigma} \frac{B_{\sigma\varsigma}}{B_{\sigma\sigma}} - 1 \right) x_\sigma x_\varsigma (\boldsymbol{u}_\varsigma - \boldsymbol{u}_\sigma) = \boldsymbol{u}. \tag{30}$$

Asymptotic analysis of AAP model

- Let us consider a regular (Hilbert) expansion of the previous model. Collecting the leading terms of the momentum equation yields

$$\lambda_\sigma \rho_\sigma^{(0)} [\boldsymbol{u}_\sigma^{*(1)} - \boldsymbol{u}_\sigma^{(1)}] = \nabla p_\sigma^{(0)}, \tag{31}$$

  where $p_\sigma^{(k)} = \varphi_\sigma \rho_\sigma^{(k)}/3$.
- If λ_σ is selected as $\lambda_\sigma = p\, B_{\sigma\sigma}/\rho$, then the previous expression becomes

$$1/p^{(0)}\, \nabla p_\sigma^{(0)} = \sum_\varsigma B_{\sigma\varsigma}\, y_\sigma y_\varsigma [\boldsymbol{u}_\varsigma^{(1)} - \boldsymbol{u}_\sigma^{(1)}], \tag{32}$$

  which clearly proves that the leading terms of the macroscopic equations recovered by means of the AAP model are consistent with Maxwell-Stefan model

Indifferentiability Principle

- If $m_\sigma = m$ for $\forall\sigma$, then $\boldsymbol{u}^*_\sigma = \boldsymbol{u}$ (Property 1) and, according to the selected tuning strategy, $\lambda_\sigma = \lambda = p\, B_{mm}/\rho$.
- Hence summing over all the species yields

$$\partial_t f + \boldsymbol{\xi}\cdot\boldsymbol{\nabla} f = \lambda \left[f_{(m)} - f \right], \tag{33}$$

where $f = \sum_\sigma f_\sigma$ and $f_{(m)}$ is defined by

$$f_{(m)} = \frac{\rho}{(2\pi\varphi/3)} \exp\left[-\frac{3\,(\boldsymbol{\xi} - \boldsymbol{u})^2}{2\,\varphi} \right]. \tag{34}$$

- This clearly proves that the AAP model satisfies the Indifferentiability Principle.

Continuous equilibrium moments

- Let us introduce the following function

$$f_e(\rho, \varphi, u_1, u_2) = \frac{\rho}{(2\pi\varphi/3)} \exp\left[-\frac{3\,(\boldsymbol{\xi}-\boldsymbol{u})^2}{2\,\varphi}\right]. \qquad (35)$$

- Let us define $\ll \cdot \gg = \int_{-\infty}^{+\infty} \cdot\, d\xi_1 d\xi_2$ and the generic moment $m_{pq} = \ll f_e\, \xi_1^p \xi_2^q \gg$.
- All the equilibrium moments appearing in the Euler system of equations are the following m_{00}, m_{10}, m_{01}, m_{20}, m_{02}, m_{11}. Unfortunately this set is made of 6 elements, but the dimension of the considered lattice (for symmetry reasons) is 9. Hence other 3 (=9-6) target equilibrium moments are missing. Arbitrarily they are selected as m_{21}, m_{12} and m_{22}.

Simplified continuous equilibrium moments

- Collecting the previous results yields

$$\begin{aligned}\bar{m}_c(\rho,\varphi,u_1,u_2) \quad = \quad & \rho\,[1,u_1,u_2,\\ & u_1^2+\varphi/3,u_2^2+\varphi/3,u_1u_2,\\ & u_1\,u_2^2+u_1\varphi/3,u_1^2\,u_2+u_2\varphi/3,\\ & \varphi\,(u_1^2u_2^2+u_1^2\varphi/3+u_2^2\varphi/3+\varphi/9)]^T.\end{aligned}$$

- The previous analytical results involve high order terms (like $u_1\,u_2^2$) which are not strictly required, in order to recover the macroscopic equations we are interested in.

$$\begin{aligned}m_c(\rho,\varphi,u_1,u_2) \quad = \quad & \rho\,[1,u_1,u_2,\\ & u_1^2+\varphi/3,u_2^2+\varphi/3,u_1u_2,\\ & u_1/3,u_2/3,\\ & (u_1^2+u_2^2)/3+\varphi/9]^T\end{aligned}$$

(3) Design of discrete local equilibrium

- On the selected lattice, the discrete integrals $m_{\sigma(*)}$, corresponding to the previous continuous ones, can be computed by means of simple linear combinations of the discrete equilibrium distribution function $f_{\sigma(*)}$ (still unknown), namely $m_{\sigma(*)} = M f_{\sigma(*)}$ where M is a matrix defined as

$$M = [1, V_1, V_2, V_1^2, V_2^2, V_1 V_2, V_1 V_2^2, V_1^2 V_2, V_1^2 V_2^2]^T. \qquad (36)$$

- We design the discrete local equilibrium such as $m_{\sigma(*)} = m_c(\rho_\sigma, \varphi_\sigma, u^*_{\sigma 1}, u^*_{\sigma 2})$, or equivalently $f_{\sigma(*)} = M^{-1} m_c(\rho_\sigma, \varphi_\sigma, u^*_{\sigma 1}, u^*_{\sigma 2})$. In particular the latter provides the operative formula for defining the local equilibrium and consequently the scheme.

Asymptotic analysis of LBM scheme

- Let us consider a regular (Hilbert) expansion of the previous model. Collecting the leading terms of the continuity equation yields

$$\partial_t \rho_\sigma^{(0)} + \boldsymbol{\nabla} \cdot [\rho_\sigma^{(0)} \boldsymbol{u}_\sigma^{*(1)}] = \omega_\sigma \nabla^2 p_\sigma^{(0)}, \tag{37}$$

  and applying the flux definition yields

$$\partial_t \rho_\sigma^{(0)} + \boldsymbol{\nabla} \cdot [\rho_\sigma^{(0)} \boldsymbol{u}_\sigma^{(1)}] = (\omega_\sigma - \tau_\sigma) \nabla^2 p_\sigma^{(0)} = -1/2 \nabla^2 p_\sigma^{(0)} \neq 0. \tag{38}$$

- The simple scheme does not preserve the mass continuity for the single species. Clearly this is due to the low accuracy of the forward Euler integration rule.
- The problem can be fixed by means of a variable transformation $f_\sigma \rightarrow \bar{f}_\sigma$ which is equivalent to apply the Crack-Nicholson integration rule.

Passive scalar (no barycentric dynamics)

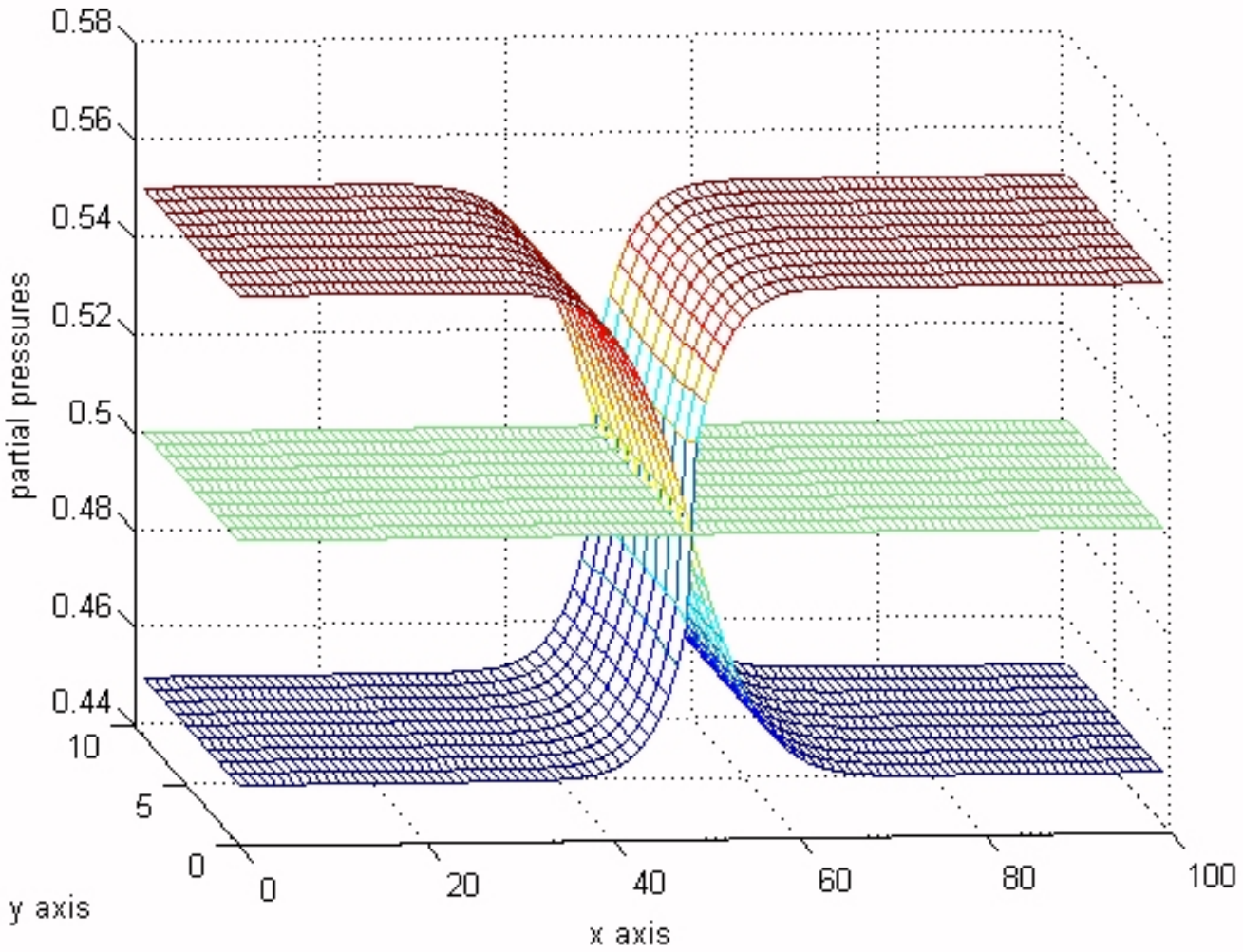

Fick model (with barycentric dynamics)

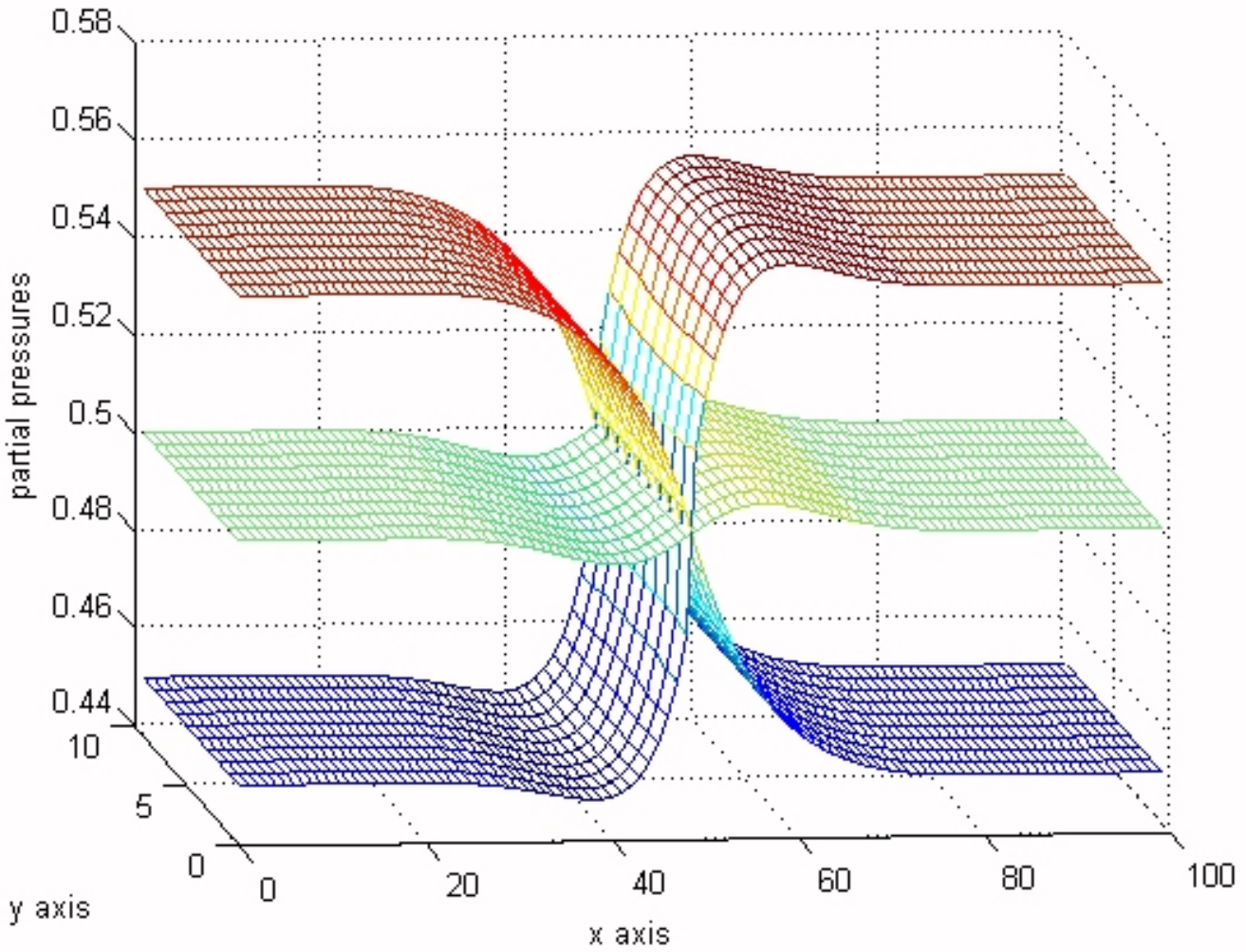

Maxwell-Stefan model (with barycentric dynamics)

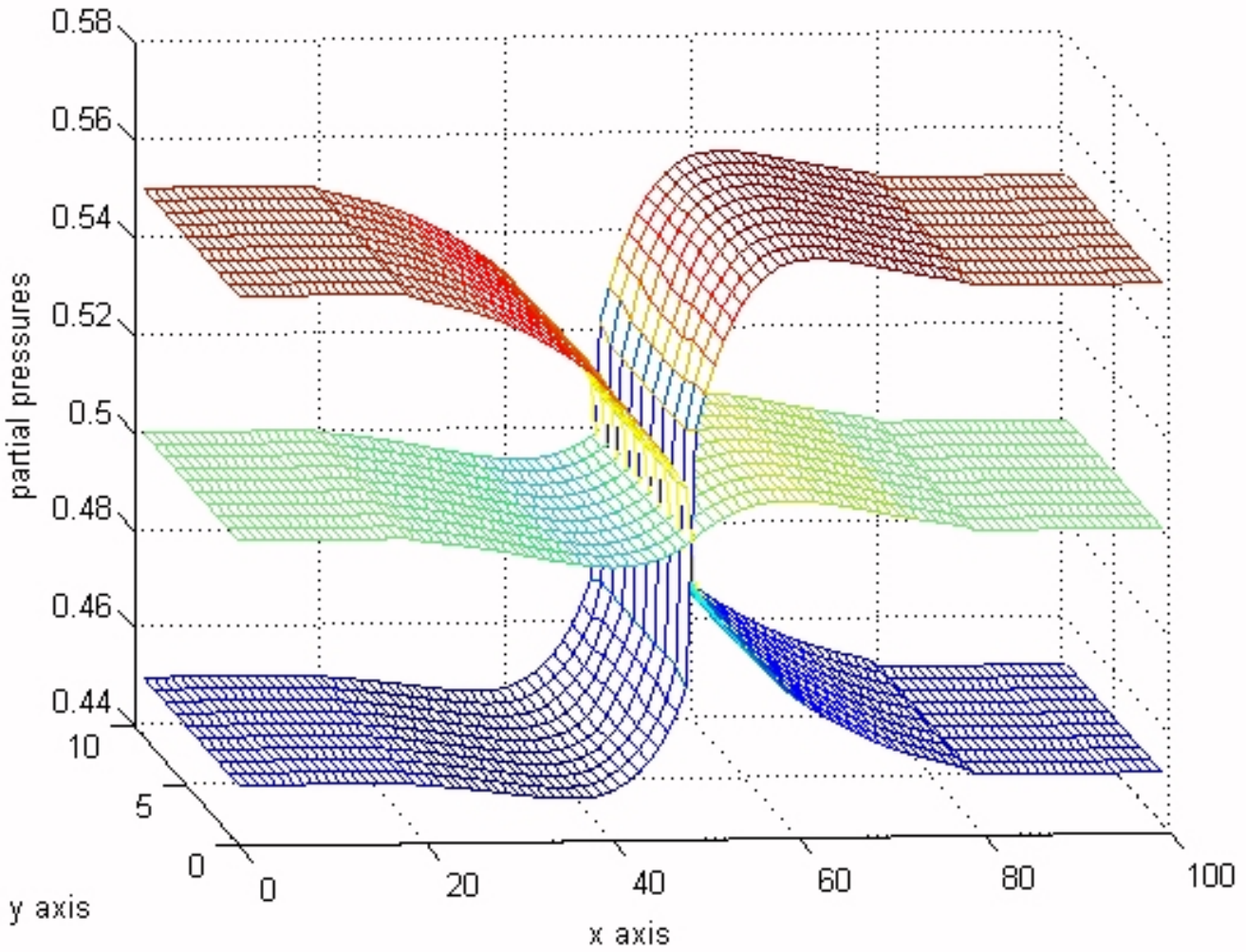

Results due to Fick and Maxwell-Stefan are similar

- Actually it seems as there is no much qualitative difference between truly Fick model and Maxwell-Stefan model.
- Let us compare directly the two models, namely

$$(\nabla y_\sigma)_F = \frac{y_\sigma}{D_\sigma}(\boldsymbol{v} - \boldsymbol{u}_\sigma) = \sum_\varsigma \frac{y_\sigma y_\varsigma}{D_\sigma}(\boldsymbol{u}_\varsigma - \boldsymbol{u}_\sigma), \tag{39}$$

$$(\nabla y_\sigma)_{MS} = \sum_\varsigma B_{\sigma\varsigma} y_\sigma y_\varsigma (\boldsymbol{u}_\varsigma - \boldsymbol{u}_\sigma). \tag{40}$$

- The difference is not in the structure of the expressions, but only in the transport coefficients: D_σ depends only on species σ, while $B_{\sigma\varsigma}$ depends on the interacting couple.
- Passive scalar approach reduces a lot the potentiality of Fick model, by simplifying the connection among species.

Conclusions: why mesoscopic methods

- Mesoscopic numerical methods inherit the (conceptual) simplicity of kinetic formulation:
  1. they involve simple transport equations because the microscopic velocities are constrained on a lattice;
  2. in the pseudo-kinetic equations of these schemes, only linear differential operators appear;
  3. the non-linearities are concentrated in the definition of the local equilibrium.
- By improving the accuracy of the numerical discretization, it is possible to tune locally the scheme in order to realize hybrid (kinetic –fluidynamic) solvers.
- Numerical error preserves some flavors of the high-order kinetic dynamics $\rightarrow$ this makes the error somehow more predictable because it is physically based.

Acknowledgments

Prof. T. Ohwada – Department of Aeronautics and Astronautics, Graduate School of Engineering Kyoto University (Japan)

Prof. L.-S. Luo – Department of Mathematics and Statistics, Old Dominion University and National Institute of Aerospace (VA, U.S.A.)

Prof. M. Calì, Prof. R. Borchiellini – Department of Energetics, Politecnico di Torino, Italy